

Validation of the Pulse Tube Refrigerator Model against a Lockheed pulse tube cooler

S.W.K. Yuan

Research and Development Division, Lockheed Martin Missiles and Space Co., Palo Alto, CA 94304, USA

A third-order computer model has been developed by modifying the Stirling Refrigerator Performance Model (SRPM), which has been validated extensively by various Stirling refrigerators in the literature. The resulting computer program, known as the Pulse Tube Refrigerator Model (PTRM), has been validated by two different pulse tube coolers. The results for the validation of a large laboratory pulse tube refrigerator built by the National Institute of Standards and Technology will be reported elsewhere. In this paper, the predicted performance of a pulse tube cooler developed by Lockheed in 1987-88 is compared with the experimental data. Good agreement was found between the two. Published by Elsevier Science Limited

Keywords: pulse tube; Stirling refrigerators; numerical models; cryocoolers

A Pulse Tube Refrigerator Model (PTRM) has been developed by modifying the Stirling Refrigerator Performance Model (SRPM), which has been validated against various Stirling coolers in the literature. They include the Lucas-Lockheed 60 K unit¹, the NASA/Philips magnetic bearing unit², the Oxford refrigerator³ and the Astronomic Infrared Sounder (AIRS) units A, B and C. A detailed description of the model can be found in reference 4. The validation of the model against a pulse tube cooler is reported in reference 5. In this report, the validation of the PTRM against a Lockheed in-house-built pulse tube cooler (PTC) will be discussed. *Figure 1* is a schematic diagram of the nodal network used in the PTRM.

Experimental apparatus

An experimental apparatus was constructed under Lockheed's Independent Research Program. This apparatus utilized a metal bellows compressor which produced a sinusoidal pressure wave with a 28 Hz frequency as the prime mover to the pulse tube. A schematic of the apparatus is depicted in *Figure 2*. The important dimensions of this pulse tube are summarized in *Table 1*. Cooling coils were used at both the hot end of the regenerator and the hot end of the pulse tube. The coldtip of the PTC consisted of a U-shaped copper tube, which provides a nearly isothermal section in which heat can be dissipated by a heater. The extension of the pulse tube includes a variable orifice valve followed by a 1-litre surge volume.

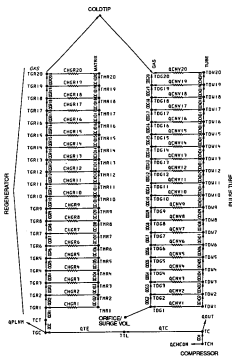


Figure 1 Schematic of nodal network diagram

Results and discussion

Figure 3a shows the predicted value of the net cooling *versus* the orifice opening (between the pulse tube and the

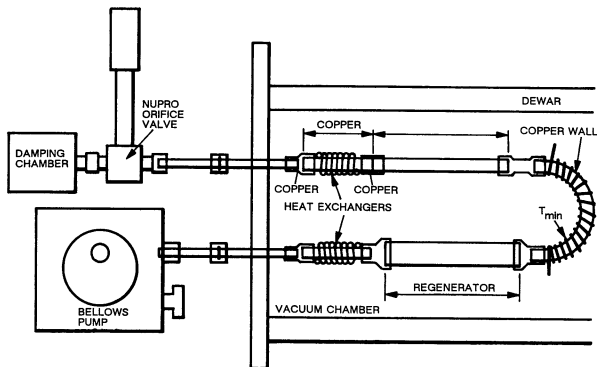


Figure 2 Schematic of Lockheed in-house-built pulse tube

Table 1 Dimensions of the Lockheed in-house-built pulse tube cooler

Compressor		
Swept volume (cm ³)	18	
Pulse tube		
O.D. (cm)	1.0	
Length (cm)	25.4	
Regenerator		
O.D. (cm)	1.9	
Length (cm)	10.0	
Wall thickness (cm)	0.05	
Mesh size	150	
Mesh material	Bronze	
Orifice		
Diameter (cm)	0.2	
Surge volume		
Volume (cm ³)	1000	
Tube housing orifice		
Diameter (cm)	0.2	
Length (cm)	1.0	

surge volume). For the sake of simplicity, it was assumed that the valve opening remains circular as the flow area of the valve is varied. This is a more generic way of modelling the flow compared to matching the flow coefficient of the valve to valve settings (which is a function of the valve type). To conserve simulation time, the coldtip temperature of each run was held at 160 K. An alternative way of running the program is to set a fixed heat load and allow the coldtip temperature to drift. However, the latter approach tends to consume much more run time. Results at constant coldtip temperature are compared to the experimental data in Figure 3b, in which the coldtip temperature is plotted as a function of the valve setting (of a Nupro valve), for various operating frequencies. An optimum valve setting close to the middle range can clearly be seen. It is interesting to

compare the prediction at 20 Hz with the experimental data of 19 Hz. At the optimum valve setting, the temperature in the experiment went down to slightly above 160 K, with no load. This agrees well with the prediction of about 0.5 W cooling at 160 K. The model is more optimistic, as losses such as streaming loss are not included in the computer program. The model also shows an optimum frequency between 10 and 20 Hz. At low frequencies, both the model and the experimental data show degraded performance. Another interesting point to note is that as the frequency is decreased the optimum performance (lowest temperature or maximum cooling) occurs at a smaller orifice size for both the experimental data and the prediction.

Figures 4–14 show some of the output parameters of the PTRM as a function of run time. Figures 4b–14b show the baseline case of 20 Hz and an orifice opening of 0.1 cm. This has been found to be the optimal opening condition. The results in Figures a and c of each figure represent the condition of 20 Hz (frequency) and 0.19 cm (orifice size), and 30 Hz (frequency) and 0.1 cm (orifice size), respectively. By comparing Figures a and b, one can study the effects of enlarging the orifice size, whereas comparing Figures b and c shows the effects of frequency. Figures 4a–c give the mass flow at the transfer line between the compressor and the regenerator. While the orifice opening has little effect on the flow rate, a high frequency tends to result in a high mass flow. Figures 5a–c are plots of pressure at the compressor (largest amplitude), and at the hot end and the cold end (smallest amplitude) of the regenerator. As one might expect, the pressure swing at the compressor and the hot end of the regenerator is large for the 30 Hz run (compared to 20 Hz). However, since the pressure drop along the system is also larger, the pressure swing at the cold end of the regenerator remains almost the same as that for 20 Hz. As noted for different orifice size, the difference in pressure swing tends to be more pronounced at the compressor than at the cold end of the regenerator.

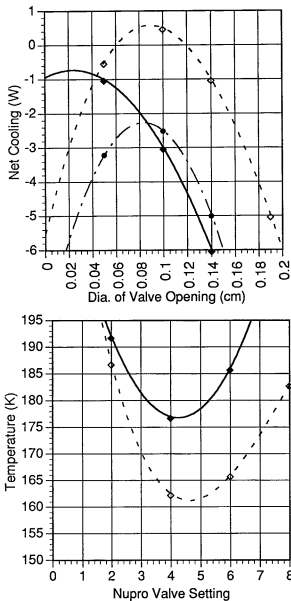


Figure 3 (a) Prediction of net cooling as a function of valve settings: \blacklozenge , 10 Hz; \circ , 20 Hz; \bullet , 30 Hz. (b) Experimental data of coldtip temperature versus valve settings: \blacklozenge , 14 Hz; \circ , 19 Hz

With an orifice size of 0.19 cm, it is difficult to pressurize the coldtip section of the pulse tube. The mass flows at three different locations in the regenerator are plotted in Figures 6a–c. Figure 6a shows a smaller distribution of the mass flow rate along the regenerator as the orifice size is increased. For the 30 Hz run, the mass flow rates are higher (Figure 6c) than for 20 Hz. The pressures at the hot and cold ends of the regenerator are plotted in Figures 7a–c. A high frequency produces a high pressure swing, whereas enlarging the orifice has the opposite effect. Figures 8a and b show the mass flow rates at three different locations in the pulse tube (the cold end has the largest amplitude). Operating at high frequency and enlarging the orifice have the same effect of increasing the flow rate. Figure 9a and b show the pressure at three different locations of the pulse tube. A large orifice size results in a diminishing pressure swing in the PTC. Due to the pressure drop, a high frequency does not translate to a large pressure swing at the pulse tube. The compressor PV diagrams are plotted in Figures 10a–c. Both operating at high frequency and enlarging the orifice result in larger PV work. A large orifice tends to fatten the PV loop while a high frequency tends to elongate the PV loop. The heat rejections from the compression space to the ambient are plotted in Figures 11a–c. As one would expect, large PV loops result in high heat rejection rates. The instantaneous heat transfers (QIP) from the coldtip to the pulse tube are plotted in Figures 12a–c. A positive value indicates that enthalpy flows from the coldtip to the pulse tube and vice versa. As one can see, a high frequency and large orifice result in a large enthalpy flow. If this quantity (QIP) is integrated, one can obtain the average enthalpy flow (QIPA). Figures 13a–c represent the average heat flow (QGEA) from the regenerator to the coldtip (i.e. at the cold end of the regenerator). This information can be used to calculate the ineffectiveness of the regenerator. For a perfect regenerator with infinite heat transfer between the matrix material and the operating gas, the net heat rate in Figure 13 is zero. Performing an energy balance around the coldtip of the PTC gives the net refrigeration ($QC = QPIA - QGEA$). Finally, the temperature profiles at three different locations along the pulse tube are plotted in Figures 14a and c. From the trade study performed, it was found that the performance is worse when the operating condition is perturbed from the baseline condition with an orifice size of 0.1 cm and

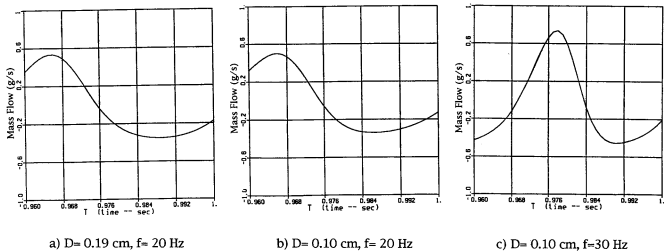


Figure 4 Mass flow in transfer line: (a) $D = 0.19$ cm, $f = 20$ Hz; (b) $D = 0.10$ cm, $f = 20$ Hz; (c) $D = 0.10$ cm, $f = 30$ Hz

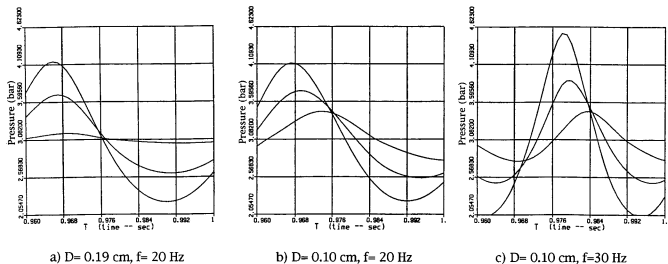


Figure 5 Pressure within cooler: (a) $D = 0.19$ cm, $f = 20$ Hz; (b) $D = 0.10$ cm, $f = 20$ Hz; (c) $D = 0.10$ cm, $f = 30$ Hz

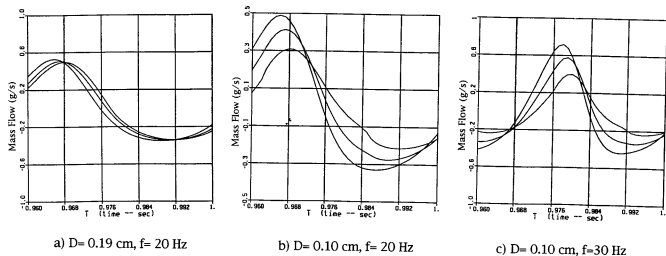


Figure 6 Mass flow in regenerator: (a) $D = 0.19$ cm, $f = 20$ Hz; (b) $D = 0.10$ cm, $f = 20$ Hz; (c) $D = 0.10$ cm, $f = 30$ Hz

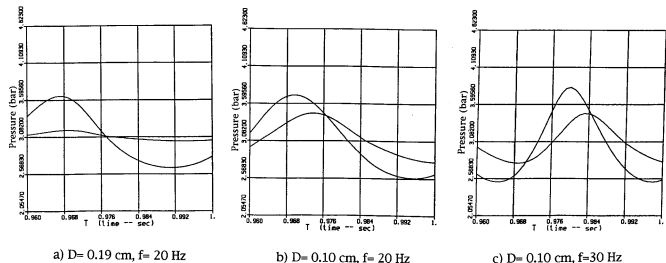


Figure 7 Pressure in regenerator: (a) $D = 0.19$ cm, $f = 20$ Hz; (b) $D = 0.10$ cm, $f = 20$ Hz; (c) $D = 0.10$ cm, $f = 30$ Hz

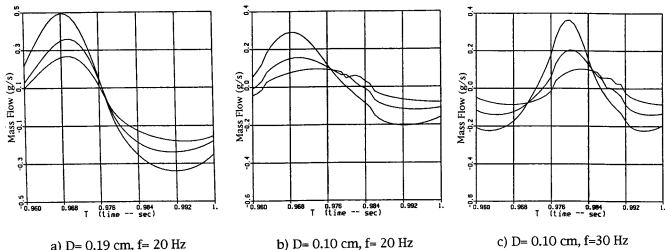


Figure 8 Mass flow in pulse tube: (a) $D = 0.19 \text{ cm}, f = 20 \text{ Hz}$; (b) $D = 0.10 \text{ cm}, f = 20 \text{ Hz}$; (c) $D = 0.10 \text{ cm}, f = 30 \text{ Hz}$

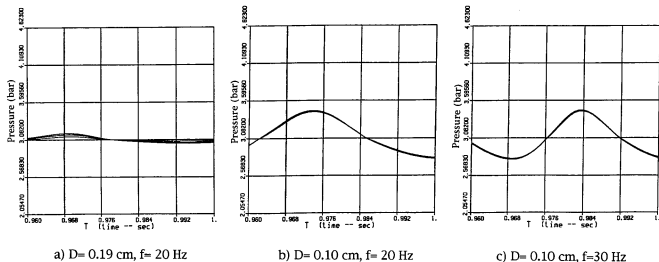


Figure 9 Pressure in pulse tube: (a) $D = 0.19 \text{ cm}, f = 20 \text{ Hz}$; (b) $D = 0.10 \text{ cm}, f = 20 \text{ Hz}$; (c) $D = 0.10 \text{ cm}, f = 30 \text{ Hz}$

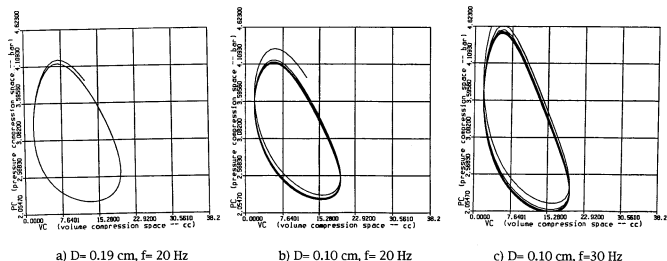


Figure 10 PV work in compressor space: (a) $D = 0.19 \text{ cm}, f = 20 \text{ Hz}$; (b) $D = 0.10 \text{ cm}, f = 20 \text{ Hz}$; (c) $D = 0.10 \text{ cm}, f = 30 \text{ Hz}$

20 Hz frequency. It is interesting to note that, for good performance, the loci of the maximum temperatures in the pulse tube tend to occur at different times (Figure 14b). However, for runs with poor performance (Figure 14a), the loci tend to coincide with each other.

The PTRM model helps to shed light on the way a pulse tube operates. An optimal operating frequency is found in PTCs as in the case of Stirling coolers. Too high a frequency tends to result in excessive pressure drop and heating which degrades the performance. An optimum orifice

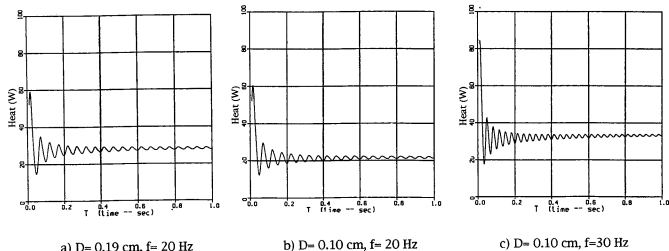


Figure 11 Heat rejection at piston head: (a) $D = 0.19$ cm, $f = 20$ Hz; (b) $D = 0.10$ cm, $f = 20$ Hz; (c) $D = 0.10$ cm, $f = 30$ Hz

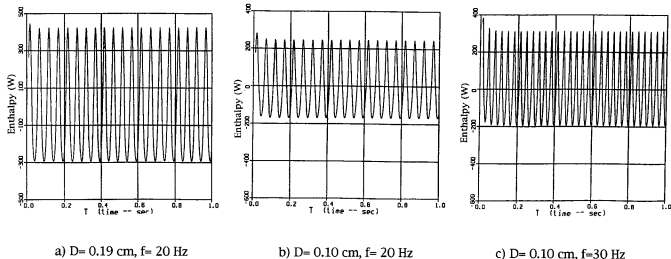


Figure 12 Instantaneous enthalpy flow in pulse tube: (a) $D = 0.19$ cm, $f = 20$ Hz; (b) $D = 0.10$ cm, $f = 20$ Hz; (c) $D = 0.10$ cm, $f = 30$ Hz

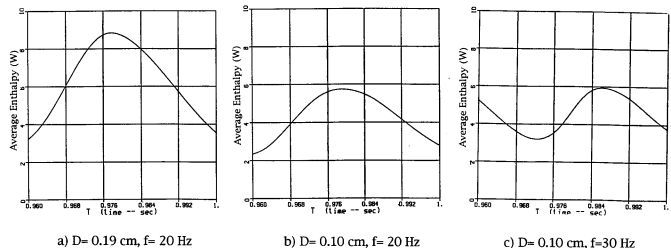


Figure 13 Average heat flow in regenerator: (a) $D = 0.19$ cm, $f = 20$ Hz; (b) $D = 0.10$ cm, $f = 20$ Hz; (c) $D = 0.10$ cm, $f = 30$ Hz

size is also required for the PTC to set up the correct phase shift between the gas in the compressor and the coldtip. A large orifice allows high mass flow in the pulse tube section (which improves performance); however, the corresponding magnitude of the pressure swing is also decreased (which degrades performance) accordingly.

Conclusions

The PTRM is validated against a Lockheed in-house-built pulse tube cooler. Good agreement was found between the experiment data and the prediction. Both the prediction and the experiment data show that the Lockheed pulse tube can

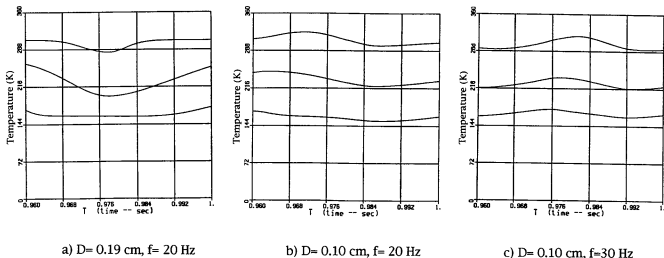


Figure 14 Gas temperature along pulse tube: (a) $D=0.19$ cm, $f=20$ Hz; (b) $D=0.10$ cm, $f=20$ Hz; (c) $D=0.10$ cm, $f=30$ Hz

be cooled down to a temperature of around 160 K. The optimum frequency of the system was predicted to be around 20 Hz, agreeing with the experimental data of 19 Hz. Moreover, both the prediction and the experimental data indicate an optimum valve opening of about the mid-range. The model also serves as a useful tool in understanding the theory behind the pulse tube cooler.

References

- 1 Yuan, S.W.K., Spradley, I.E., Yang, P.M. and Nast, T.C. Computer simulation model for Lucas Stirling refrigerators *Cryogenics* (1992) **32** 143–148
- 2 Yuan, S.W.K. and Spradley, I.E. Validation of the Stirling refrigerator performance model against the Phillips/NASA magnetic bearing refrigerator *Proc 7th Int Cryocooler Conf* Vol 1, Phillips Labs, USA (1993) 280
- 3 Yuan, S.W.K. and Spradley, I.E. Validation of the Stirling refrigerator performance model against the Oxford refrigerator *Adv Cryog Eng* (1994) **39B** 1359–1365
- 4 Yuan, S.W.K. and Spradley, I.E. A third order computer model for Stirling refrigerators *Adv Cryog Eng* (1992) **37B** 1055–1062
- 5 Yuan, S.W.K. A blind test on the Pulse Tube Refrigerator Model (PTRM), paper presented at the Cryogenic Engineering Conference, Columbus, Ohio (1995)